

Supporting Information

XAS Characterization of a Nitridoiron(IV) Complex with a Very Short Fe–N Bond

Jan-Uwe Rohde,^{†,‡} Theodore A. Betley,^{§,||} Timothy A. Jackson,[†]
Caroline T. Saouma,[§] Jonas C. Peters,[§] and Lawrence Que, Jr.[†]

[†] *Department of Chemistry and Center for Metals in Biocatalysis, University of Minnesota,
Minneapolis, MN 55455, USA*

[‡] *Current address: Department of Chemistry, The University of Iowa, Iowa City, IA 52242, USA*

[§] *Department of Chemistry and Chemical Engineering, Arnold and Mabel Beckman Laboratories
of Chemical Synthesis, California Institute of Technology, Pasadena, CA 91125, USA*

^{||} *Current address: Department of Chemistry, Massachusetts Institute of Technology, Cambridge,
MA 02139, USA*

page

- S3** **Table S1.** XAS pre-edge peak energies and intensities.
- S4** **Figure S1.** Fe K-edge EXAFS spectra ($k^3\chi(k)$) of **1**, **2**, **3**, and three samples of **4**.
- S5** **Table S2.** EXAFS fitting results for **2**, **3**, and **1**.
- S5** **Table S3.** Distances in **2**, **3**, and **1** revealed by crystal structure determination.
- S6** **Figure S2.** Fourier transform of the Fe K-edge EXAFS data and Fourier-filtered EXAFS spectrum of $[\text{PhBP}^{i\text{Pr}}_3]\text{Fe}(\text{NPh}_2)$, **2**; experimental data and best fit.
- S6** **Figure S3.** Fourier transform of the Fe K-edge EXAFS data and Fourier-filtered EXAFS spectrum of $[\text{PhBP}^{i\text{Pr}}_3]\text{Fe}(\text{NAd})$, **3**; experimental data and best fit.
- S7** **Figure S4.** Fourier transform of the Fe K-edge EXAFS data and Fourier-filtered EXAFS spectrum of $\{[\text{PhBP}^{i\text{Pr}}_3]\text{Fe}\}_2(\mu\text{-N}_2)$, **1**; experimental data and best fit.
- S8** **Table S4.** EXAFS fitting results for a sample of **4** (**4A**, $[\text{Fe}] = 0.01 \text{ M}$).
- S9** **Table S5.** EXAFS fitting results for a second sample of **4** (**4B**, $[\text{Fe}] = 0.03 \text{ M}$).
- S10** **Figure S5.** Fourier transforms of the Fe K-edge EXAFS data and Fourier-filtered EXAFS spectra of additional samples of $[\text{PhBP}^{i\text{Pr}}_3]\text{Fe}(\text{N})$, **4** ($[\text{Fe}] = 0.03 \text{ M}$); experimental data and best fits; comparison of the Fourier transforms of the Fe K-edge EXAFS data of samples **4A** ($[\text{Fe}] = 0.01 \text{ M}$) and **4B** ($[\text{Fe}] = 0.03 \text{ M}$).
- S11** **Table S6.** EXAFS fitting results for a sample of **5** ($[\text{Fe}] = 0.035 \text{ M}$).

Table S1. XAS pre-edge peak energies and intensities for the [PhBP^{iPr}₃]Fe(N_x) complexes in this study from refinements with multiple peaks.^a

complex	E_0 (eV)	$E_{\text{pre-edge}}$ (eV)	area	$E_{\text{pre-edge}}$ (eV) (centroids)	total area
1	7117.3	7112.2	13.3	7112.6	16.8
		7113.9	3.5		
2	7119.0	7111.1	2.0	7112.4	24.5
		7112.3	17.1		
		7113.4	5.4		
3	7118.0	7111.6	7.9	7112.4	16.2
		7113.1	8.3		
4A (0.01 M Fe)	7120.2	7111.6	4.9	7113.1	64.5
		7113.2	59.6		
4B (0.03 M Fe)	7120.0	7111.7	7.7	7112.8	59.8
		7113.0	52.1		

^a E_0 is conventionally defined as the first inflection point of the Fe K-edge. Pre-edge peak intensities are reported as peak areas (normalized to the edge jump) and were multiplied by 100.

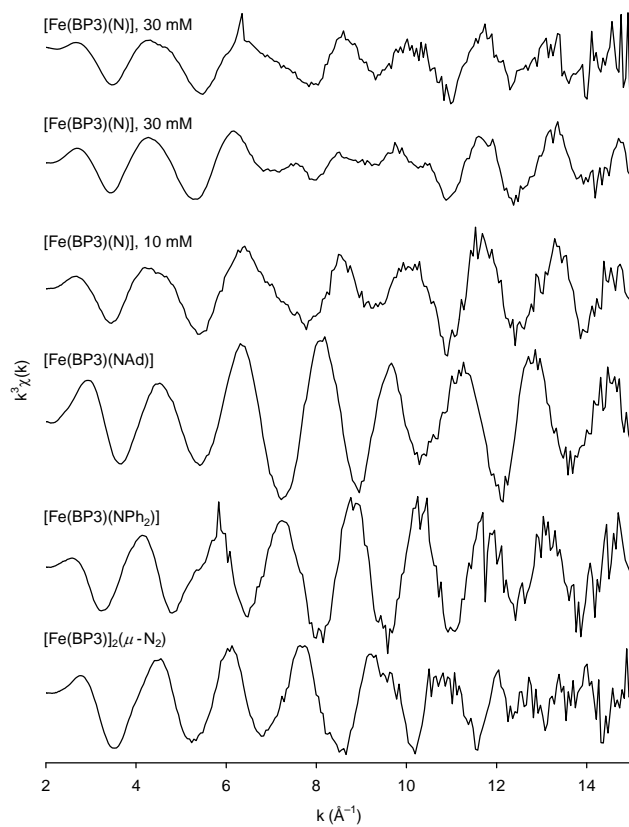


Figure S1. Fe K-edge EXAFS spectra ($k^3 \chi(k)$) of $\{[\text{PhBP}^{i\text{Pr}}_3\text{Fe}]_2(\mu\text{-N}_2)$, **1**, $[\text{PhBP}^{i\text{Pr}}_3\text{Fe}(\text{NPh}_2)$, **2**, $[\text{PhBP}^{i\text{Pr}}_3\text{Fe}(\text{NAd})$, **3**, and three samples of $[\text{PhBP}^{i\text{Pr}}_3\text{Fe}(\text{N})$, **4**.

Table S2. EXAFS fitting results for [PhBP^{iPr}₃]Fe(NPh₂), **2**, [PhBP^{iPr}₃]Fe(NAd), **3**, and {[PhBP^{iPr}₃]Fe}₂(μ-N₂), **1**.^a

Fit	Fe–N			Fe–P			Fe···C			Fe···C			GOF $\varepsilon^2 \cdot 10^3$ ^b
	<i>n</i>	<i>r</i> (Å)	$\Delta\sigma^2$	<i>n</i>	<i>r</i> (Å)	$\Delta\sigma^2$	<i>n</i>	<i>r</i> (Å)	$\Delta\sigma^2$	<i>n</i>	<i>r</i> (Å)	$\Delta\sigma^2$	
1	1	1.959	2.5	3	2.463	0.6	2	2.938	0.9				0.512
(<i>l</i>)	<i>l</i>	1.959	2.8	3	2.463	0.6	2	2.936	0.6				0.686) ^c
2	1	1.961	2.8	3	2.463	0.7							0.656
3				3	2.463	0.7	2	2.935	1.4				0.709
4				3	2.463	0.8							0.779
1	1	1.637	0.7	3	2.269	0.9	1	3.163	-2.9	3	3.443	4	0.528
(<i>l</i>)	<i>l</i>	1.636	0.8	3	2.269	0.8	<i>l</i>	3.168	-2.9	3	3.454	3.9	0.696) ^c
2	1	1.638	0.7	3	2.269	0.9	1	3.163	-3.2				0.612
3	1	1.636	0.6	3	2.269	0.9				3	3.436	1.1	0.609
4	1	1.637	0.6	3	2.269	1.0							0.668
5				3	2.268	0.8	1	3.167	-3.3	3	3.44	5	1.112
6				3	2.269	0.9							1.122
1	1	1.794	4.1	3	2.352	3.8							0.557
(<i>l</i>)	<i>l</i>	1.789	5.1	3	2.353	3.8							0.818) ^c
2				3	2.351	3.8							0.725

^a Fourier-transformed range **1**, **2**, and **3**: $k = 2-15 \text{ \AA}^{-1}$ (resolution 0.12 Å). *r* is in units Å, $\Delta\sigma^2$ in 10^3 \AA^2 . The typical error of analysis for interatomic distances (*r*) is approximately $\pm 0.02 \text{ \AA}$. ^b Back-transformation ranges for **2**: $r' = 0.80-3.80 \text{ \AA}$; for **3**: $r' = 0.60-3.80 \text{ \AA}$; and for **1**: $r' = 0.60-3.60 \text{ \AA}$. ^c Fits to unfiltered data corresponding to the best fits to filtered data.

Table S3. Distances (Å) in **2**, **3**, and **1** revealed by crystal structure determination.

	2		3		1	
	<i>d</i> (Å)	average	<i>d</i> (Å)	average	<i>d</i> (Å)	average
Fe–N	1.953		1.638		1.761–1.818 (4 x)	1.793
Fe–P	2.443 2.462 2.467	2.457	2.260 2.263 2.297	2.273	2.333–2.394 (12 x)	2.357
Fe···C ^a	2.936 2.982	2.959	3.074			
Fe···C ^b	3.434–3.733 (9 x)	3.592	3.366–3.545 (9 x)	3.45		

^a *Ips*o carbon atoms of the *N*-phenyl (**2**) and *N*-adamantyl substituents (**3**). ^b Carbon atoms adjacent to the ligating phosphorus atoms.

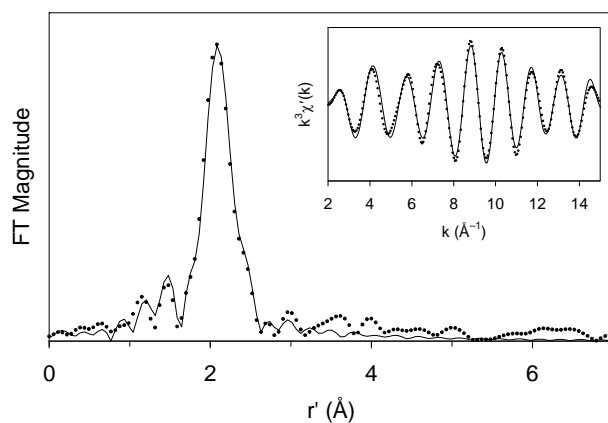


Figure S2. Fourier transform of the Fe K-edge EXAFS data ($k^3\chi(k)$) and Fourier-filtered EXAFS spectrum ($k^3\chi'(k)$, inset) of $[\text{PhBP}^{i\text{Pr}}_3]\text{Fe}(\text{NPh}_2)$, **2**, Fourier-transformed range $k = 2\text{--}15 \text{ \AA}^{-1}$; experimental data ($\bullet\bullet\bullet$) and fit 1, Table S2 (—); Back-transformation range: $r' = 0.80\text{--}3.80 \text{ \AA}$.

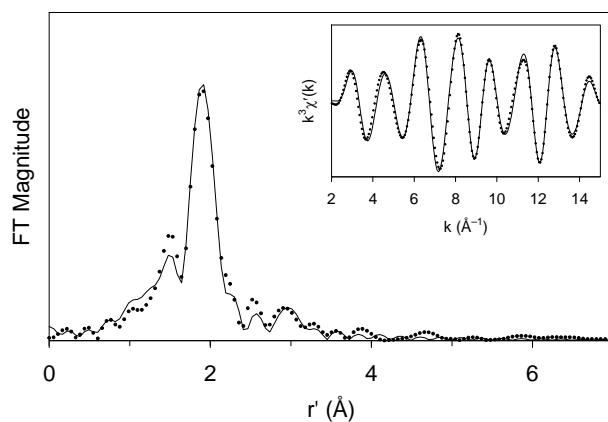


Figure S3. Fourier transform of the Fe K-edge EXAFS data ($k^3\chi(k)$) and Fourier-filtered EXAFS spectrum ($k^3\chi'(k)$, inset) of $[\text{PhBP}^{i\text{Pr}}_3]\text{Fe}(\text{NAd})$, **3**, Fourier-transformed range $k = 2\text{--}15 \text{ \AA}^{-1}$; experimental data ($\bullet\bullet\bullet$) and fit 1, Table S2 (—); Back-transformation range: $r' = 0.60\text{--}3.80 \text{ \AA}$.

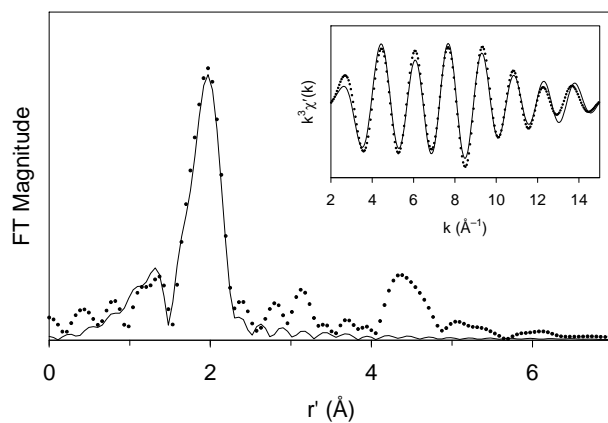


Figure S4. Fourier transform of the Fe K-edge EXAFS data ($k^3\chi(k)$) and Fourier-filtered EXAFS spectrum ($k^3\chi'(k)$, inset) of $\{[\text{PhBP}^{i\text{Pr}}_3]\text{Fe}\}_2(\mu\text{-N}_2)$, **1**, Fourier-transformed range $k = 2\text{--}15 \text{ \AA}^{-1}$; experimental data ($\bullet\bullet$) and fit 1, Table S2 (—); Back-transformation range: $r' = 0.60\text{--}3.60 \text{ \AA}$.

Table S4. EXAFS fitting results for a sample of [PhBPⁱPr₃]Fe(N), **4 (4A)**, [Fe] = 0.01 M).^a

Fit	Fe-N			Fe-N			Fe-P			Fe-P			Fe···C			GOF $\epsilon^2 \cdot 10^3$ ^b
	<i>n</i>	<i>r</i> (Å)	$\Delta\sigma^2$	<i>n</i>	<i>r</i> (Å)	$\Delta\sigma^2$	<i>n</i>	<i>r</i> (Å)	$\Delta\sigma^2$	<i>n</i>	<i>r</i> (Å)	$\Delta\sigma^2$	<i>n</i>	<i>r</i> (Å)	$\Delta\sigma^2$	
1							3	2.210	6.0							1.744
2							2	2.216	2.5	1	2.442	-0.5				0.934
3							1.5	2.210	0.3	1.5	2.434	2.7				0.885
4							1	2.203	-1.6	2	2.418	8.1				0.951
5	1	1.510	4.3				1.5	2.209	0.2	1.5	2.432	2.9				0.816
6	0.5	1.515	0.2				1.5	2.209	0.1	1.5	2.431	2.8				0.671
7				1	2.05	9	1.5	2.208	0.7	1.5	2.441	2.4				0.842
8				0.5	2.03	1	1.5	2.214	0.7	1.5	2.441	2.1				0.854
9	0.55	1.517	0.8	0.45	2.02	4	1.65	2.213	1.0	1.35	2.439	1.3				0.600
10	0.5	1.518	0.2	0.5	2.00	4	1.5	2.212	0.3	1.5	2.435	2.3				0.573
11	0.45	1.518	-0.3	0.55	1.98	3	1.35	2.211	-0.4	1.65	2.432	3.4				0.558
12	0.5	1.518	0.3	0.5	2.00	4	1.5	2.212	0.3	1.5	2.435	2.4	1	3.03	9	0.555
													3	3.470	2.2	
													3	3.71	5	
(12)	0.5	1.523	0.7	0.5	2.025	0.1	1.5	2.216	0.9	1.5	2.443	2.1	1	3.02	8	0.602) ^c
													3	3.470	1.0	
													3	3.702	3.4	
13	0.5	1.515	0.3				1.5	2.209	0.1	1.5	2.431	2.9	0.7	3.08	3	0.693
													3	3.473	2.0	
													3	3.71	4	
14				0.5	2.03	1	1.5	2.214	0.8	1.5	2.441	2.2	1	3.06	5	0.922
													3	3.47	2	
													3	3.71	4	
15							1.5	2.209	0.3	1.5	2.433	2.9	1	3.06	6	0.952
													3	3.47	2	
													3	3.71	4	

^a Fourier-transformed range: $k = 2-15 \text{ \AA}^{-1}$ (resolution 0.12 Å). r is in units Å, $\Delta\sigma^2$ in 10^3 \AA^2 . The typical error of analysis for interatomic distances (r) is approximately $\pm 0.02 \text{ \AA}$. ^b Back-transformation range: $r' = 0.60-3.80 \text{ \AA}$. ^c Fits to unfiltered data corresponding to the best fits to filtered data.

Table S5. EXAFS fitting results for a second sample of [PhBP^{iPr}₃]Fe(N), **4 (4B)**, [Fe] = 0.03 M).^a

Fit	Fe-N			Fe-N			Fe-P			Fe-P			Fe...C			GOF $\epsilon^2 \cdot 10^3$ ^b
	<i>n</i>	<i>r</i> (Å)	$\Delta\sigma^2$	<i>n</i>	<i>r</i> (Å)	$\Delta\sigma^2$	<i>n</i>	<i>r</i> (Å)	$\Delta\sigma^2$	<i>n</i>	<i>r</i> (Å)	$\Delta\sigma^2$	<i>n</i>	<i>r</i> (Å)	$\Delta\sigma^2$	
1										3	2.34	19				1.087
3							1.5	2.235	2.2	1.5	2.429	1.6				0.656
5	0.8	1.513	9				1.5	2.233	2.2	1.5	2.428	1.7				0.684
6	0.5	1.529	2.9				1.5	2.234	2.1	1.5	2.428	1.6				0.601
8				0.5	1.824	-0.6	1.5	2.239	2.7	1.5	2.434	1.8				0.685
9	0.5	1.535	3.7	0.5	1.819	-0.2	1.5	2.238	2.5	1.5	2.433	1.7				0.524
10	0.45	1.538	2.6	0.55	1.824	1.2	1.35	2.231	1.6	1.65	2.426	2.5				0.512
11	0.4	1.541	1.3	0.6	1.836	4	1.2	2.225	0.7	1.8	2.419	3.3				0.498
12	0.5	1.535	3.8	0.5	1.820	-0.2	1.5	2.237	2.4	1.5	2.432	1.7	1	3.12	0	0.559
													3	3.47	6	
													3	3.73	6	
(12)	0.5	1.535	3.7	0.5	1.817	-0.3	1.5	2.240	2.6	1.5	2.435	1.6	1	3.113	1.1	0.551) ^c
													3	3.490	6.9	
													3	3.743	6.4	
13	0.5	1.528	3.0				1.5	2.234	2.0	1.5	2.428	1.5	1	3.12	0	0.657
													3	3.48	6	
													3	3.73	6	
14				0.5	1.826	-0.6	1.5	2.238	2.6	1.5	2.433	1.7	1	3.12	0	0.751
													3	3.47	6	
													3	3.73	6	
15							1.5	2.234	2.1	1.5	2.429	1.6	1	3.12	0	0.709
													3	3.48	6	
													3	3.73	6	

^a Fourier-transformed range: $k = 2-15 \text{ \AA}^{-1}$ (resolution 0.12 Å). r is in units Å, $\Delta\sigma^2$ in 10^3 \AA^2 . The typical error of analysis for interatomic distances (r) is approximately $\pm 0.02 \text{ \AA}$. ^b Back-transformation range: $r' = 0.60-3.80 \text{ \AA}$. ^c Fits to unfiltered data corresponding to the best fits to filtered data.

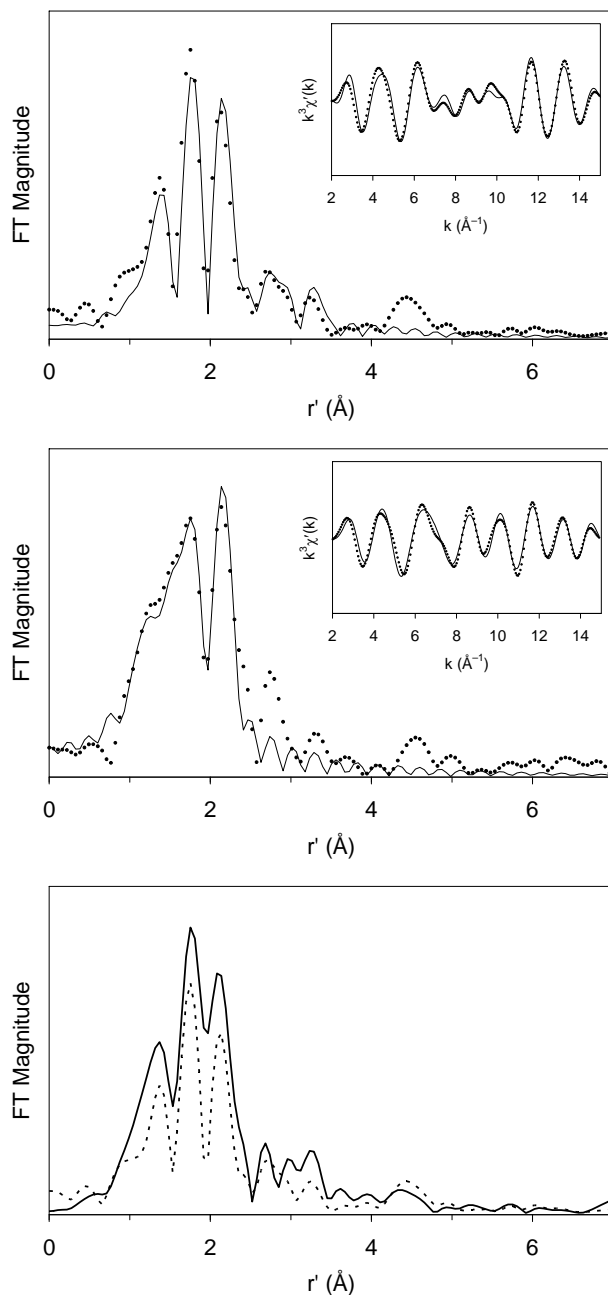


Figure S5. Fourier transforms of the Fe K-edge EXAFS data ($k^3\chi(k)$) and Fourier-filtered EXAFS spectra ($k^3\chi'(k)$, inset) of additional samples of $[\text{PhBP}^{\text{Pr}}_3]\text{Fe}(\text{N})$, **4** ($[\text{Fe}] = 0.03 \text{ M}$); top, **4B**, Fourier-transformed range $k = 2\text{--}15 \text{ \AA}^{-1}$; experimental data ($\bullet\bullet$) and fit 12, Table S5 (—); Back-transformation range: $r' = 0.60\text{--}3.80 \text{ \AA}$; middle, **4C**, Fourier-transformed range $k = 2\text{--}14.9 \text{ \AA}^{-1}$; experimental data ($\bullet\bullet$) and fit 4c, Table 2 (—); Back-transformation range: $r' = 0.60\text{--}3.60 \text{ \AA}$; bottom, comparison of the Fourier transforms of the Fe K-edge EXAFS data ($k^3\chi(k)$) of samples **4A** (—, $[\text{Fe}] = 0.01 \text{ M}$) and **4B** (---, $[\text{Fe}] = 0.03 \text{ M}$).

Table S6. EXAFS fitting results for a sample of [PhBP^{CH₂Cy}₃]Fe(N), **5** ([Fe] = 0.035 M).^a

Fit	Fe-N			Fe-P			GOF ^b
	<i>n</i>	<i>r</i> (Å)	σ^2	<i>n</i>	<i>r</i> (Å)	σ^2	
1				5	2.18	6.0	0.547
2				4	2.18	4.1	0.512
3				3	2.19	2.3	0.486
4				2	2.19	0.6	0.472
5	1	1.56	7.9	4	2.19	4.2	0.649
6	1	1.55	8.1	3	2.19	2.4	0.548
7	1	1.55	7.4	2	2.19	0.6	0.455
8	0.8	1.56	4.2	2	2.19	0.6	0.452
9	0.7	1.55	3.8	2.1	2.19	0.8	0.458
10	0.8	1.56	4.7	2.4	2.19	1.3	0.486
							GOF ^b
11				4	2.19	4.2	0.962
12				3	2.19	3.9	0.653
13				2	2.18	3.2	0.483
14	1	1.55	8.1	3	2.19	2.4	0.470
15	1	1.56	7.7	2	2.19	0.6	0.340
16	0.8	1.55	6.8	2	2.19	1.3	0.325

^a Fourier-transformed range: $k = 2-15 \text{ \AA}^{-1}$ (resolution 0.12 Å). r is in units Å, σ^2 in 10^3 \AA^2 . The typical error of analysis for interatomic distances (r) is approximately $\pm 0.02 \text{ \AA}$. ^b GOF = $[\sum k^6(\chi_{\text{exptl}} - \chi_{\text{sim}})^2 / \sum k^6 \chi_{\text{exptl}}^2]^{1/2}$. Fits 1–10 are to unfiltered $k^3\chi(k)$ EXAFS data, fits 11–16 to unfiltered $k\chi(k)$ EXAFS data.